FERMILAB-Proposal-0735

PURDUE UNIVERSITY DEPARTMENT OF PHYSICS

April 11, 1983

Dr. Norman Gelfand
Director's Office
Fermilab
Batavia, IL 60510

Dear Norman:

Enclosed are 20 copies of the D0 proposal we discussed with you one month ago, as promised it is modest in size but "big" in physics.

We are proposing a search for quark-gluon plasmas produced in $\bar{p}p$ collisions at $\sqrt{s}$ = 2 TeV. QCD experts are convinced that at high enough energy density (> 2 GeV/f^3) there exists a deconfined quark-gluon phase of hadronic matter. Bjorken has pointed out (Fermilab-Pub-82/59-THY) that the large yield of non jet-like events in $\bar{p}p$ data from the SPS with transverse energy (E_t) ~ 60 GeV may imply energy densities in the 10-50 GeV/f^3 region!! More recently Van Hove has interpreted (P.L. 118B, 138) the $\bar{p}p$ SPS data on $\langle P_t \rangle$ - vs - multiplicity as a possible signal for the deconfinement phase transition in hadronic matter.

We are proposing an experiment that will look in the central region ($|y|<3$) for three signatures of the phase transition. The basic idea is to look for characteristic changes in (1) $\langle P_t \rangle$, (2) particle composition, and (3) low-mass dileptons as a function of charged particle multiplicity. The temperature of the quark-gluon plasma is of the order of 200 MeV, hence one looks at low energy particles, P_t<1 GeV/c. Furthermore, the measured cross sections for the high E_t events are relatively large, of the order of 1 μb, about 100-1000 times larger than the cross section for single jets of the same E_t. We believe that the simultaneous observation of all three signatures would unambiguously establish the existence of the deconfined phase - one of the fundamental predictions of QCD.

As a consequence of the large cross sections and of operating in the low P_t range of the particle spectrum, the apparatus of the experiment is rather modest compared to that of the typical D0 proposal. The spectrometer weighs ~10 tons and occupies a volume 6m wide by 2m high by 6m along the beam. Several other noteworthy features of the proposal are:

Physics Building
West Lafayette, Indiana 47907

38 pp.

1. Luminosity requirement of 10^{27} $cm^{-2}sec^{-1}$.

2. No Main Ring overpass required.

3. Apparatus relatively easy to install.

4. Cost estimate of less than $2M.

For the reasons outlined above we feel that this proposal makes an ideal first-round experiment for the D0 area. It addresses in a novel way a new and fundamental area of particle physics with an apparatus which is well matched to the capabilities of the D0 environment.

We apologize for the lateness of this submittal, our excuse being that the genesis of this proposal arose from very recent physics developments.

Sincerely,

L. Gutay

L. Gutay, Purdue

R.P. Scharenberg

R.P. Scharenberg, Purdue

Frank Turkot

F. Turkot, Fermilab

Duane Carmony

D. Carmony, Purdue

P.S. We might point out that we are not entirely neophytes in this area of physics, our CO result (E-591) on the power-law yield of nuclear fragments also has the "smell" of a phase transition (P.L. 118B, 458, 1982). Also we were the first to determine the Hagedorn limiting temperature (PRL 38, 1, 1977) and the size a la Hanbury-Twiss (PRL 38, 873, 1977) of the centrally produced hadronic matter.

SEARCH FOR A DECONFINED QUARK GLUON PHASE OF STRONGLY INTERACTING MATTER IN $\bar{p}$-p INTERACTIONS AT $\sqrt{s} \simeq 2$ TeV

Submitted by Scientists at Purdue University
and the Fermi National Accelerator Laboratory

Abstract

We propose to use a double arm magnetic spectrometer and a central tracking chamber located at the DØ intersection area that can utilize low, from 10^{27} to $10^{28}\text{cm}^{-2}\text{sec}^{-1}$, luminosity to measure the transverse momentum distributions dN/dp_t up to $p_t = 1.0$ GeV/c for centrally produced $p^{\pm},\pi^{\pm},e^{\pm}$ as a function of the charged particle multiplicity n_c. The temperature T and the size of centrally produced plasma can be extracted from the transverse momentum (p_t) distributions dN/dp_t and from the like pion correlations, respectively.

Evidence for a quark gluon plasma manifests itself by

(a) Breaks in $\langle p_t \rangle$ as a function of dn_c/dy in the central region $|y| \leq 1$.

(b) Changes in the particle composition as a function of the charged particle multiplicity n_c.

(c) Onset of low mass dilepton pair production as a function of the charged particle multiplicity n_c.

We also propose to measure the ratio of the gamma-ray multiplicity n_γ to charged particle multiplicity n_c for high multiplicity events. Evidence for a Centauro event, if produced in the central region, would manifest itself by high charged particle multiplicities $n_c \simeq 30$ with the number of n_γ consistent with zero.

Because we momentum analyze only low energy particles in observing these signatures, the size and complexity of this apparatus is one tenth of that required for a 4π detector which studies high transverse momentum reactions.

Person to contact: L. J. Gutay
Commercial phone: (317) 494-5047
FTS phone: 331-2084

Names of the Experimenters

Members of Purdue University:

Professors:	D. D. Carmony
	A. S. Hirsch
	L. J. Gutay
	N. T. Porile
	R. P. Scharenberg
	B. C. Stringfellow
Research Associates:	A. Bujak
	Z. Seres
Students:	C. Sangster
	F. Poole

Members of Fermi National Accelerator Laboratory:

Physicist:	F. Turkot

I. Introduction

Although the original models for particle production were statistical and thermodynamic in nature (Fermi[1] and Landau[2]), the main thrust of high energy physics has been the study of particles and resonances. The fact that these have definite quantum numbers and could be classified into various representations of symmetry groups by Gell-Mann[3] as well as the existence of Bjorken scaling[4] has led to the hypothesis that hadrons are made of quarks and gluons.

The absence of any evidence for the existence of free quarks has led to the concept of quark confinement. From the concept of asymptotic freedom[5] QCD evolved[6] as the theory of strong interactions in agreement with numerous hard scattering experiments. Lattice gauge calculations of QCD predict a phase transition from hadrons to a quark-gluon plasma at sufficiently high temperatures and/or quark densities.[7] There is a general theoretical concensus that temperatures of $T \sim 200$ MeV and/or quark antiquark densities of $n_q + \bar{n}_q = 2$ to 4 per cubic fermi are required to produce a quark-gluon plasma.[8] Such a density may be thought of as two protons being "placed on top of each other."

There are strong experimental indications from the CERN UA1[9] collaboration that such temperatures may be produced in high multiplicity collisions at $\sqrt{s} = 0.54$ TeV. Evidence for thermalization at lower temperature $T = 120$ MeV suggests that it is likely that temperatures $T > 200$ MeV (see Section II) and quark densities > 2 to 4 per cubic fermi (see Appendix I) are attainable in high multiplicity $n_c > 50$ collisions at $\sqrt{s} = 2$ TeV.

The energy density vs. T for a phase transition[10] from SU_2 lattice gauge calculations is shown in Fig. 1 for a gluon plasma. Similar results have been obtained from lattice gauge calculations using SU_3 color fields.[11] To cast Fig. 1 into a form that can be related to experimental quantities we divide the y axis of Fig. 1 by T. The general shape remains unchanged as shown in Fig. 2 where we introduced the symbol $\sigma = \frac{\varepsilon}{T}$, the entropy density. According to statistical mechanics and thermodynamics, the entropy density is proportional to the rate of particle production over a unit rapidity ($\sigma \propto \frac{dn}{dy}$) and the temperature is proportional to the average transverse

momentum ($T \propto \langle p_t \rangle$). Thus from the above relations and Fig. 2 we can deduce the shape of dn/dy as a function of $\langle p_t \rangle$ as shown in Fig. 3. As discussed in the next section (II), it is possible to quantitatively calibrate $\langle p_t \rangle$ versus T so that the critical (deconfinement) temperature could be determined. That means dn_c/dp_t for pions must be a Bose-Einstein distribution in the range $p_t \leq 1.0$ GeV/c. Then it should be possible to speak of a thermalized energy density.

From the study of high transverse energy jets, Bjorken[8] concluded that energy densities well above the expected phase transition energy densities may exist, already at the CERN $\bar{p}$-p collider energies.

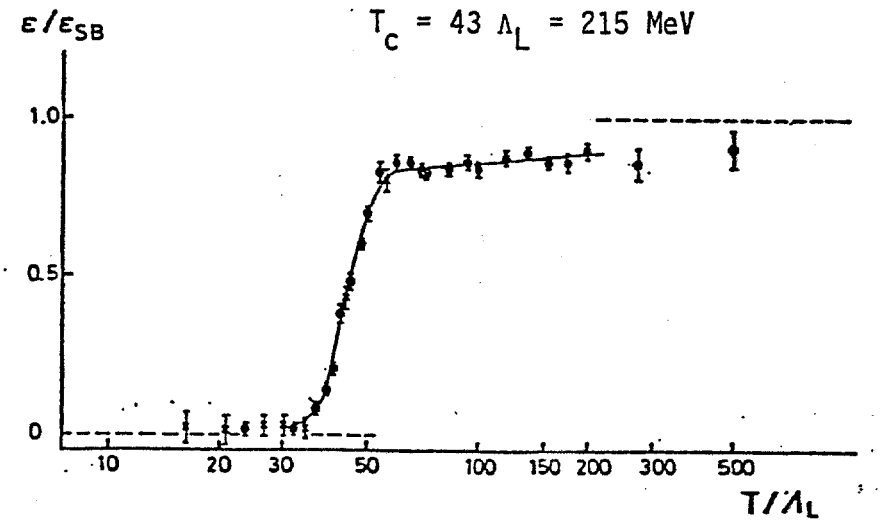

Fig. 1. Theoretical prediction for the energy density as function of temperature for a gluon plasma from Ref. 10. (Sharpness enhanced by log plot.)

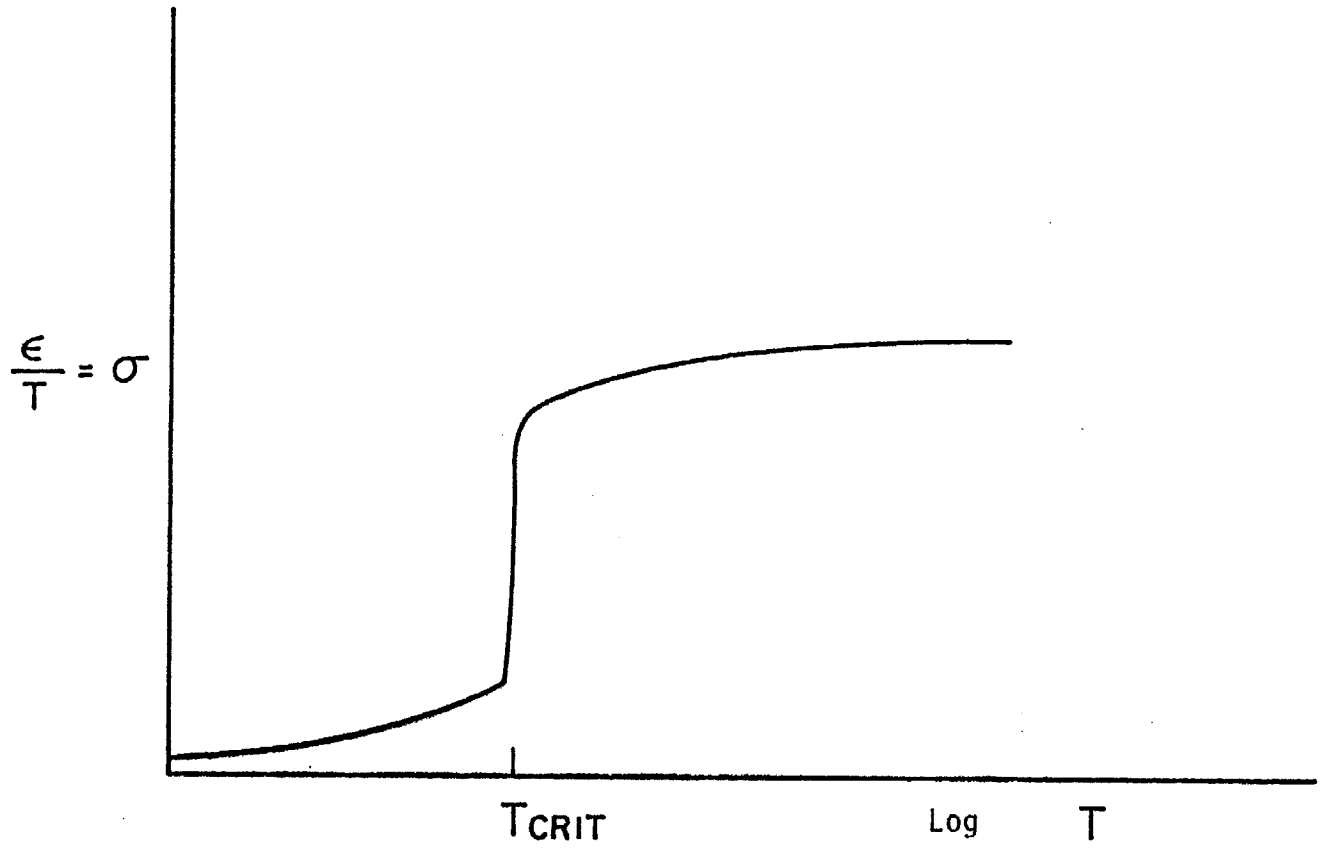

Fig. 2. Theoretical prediction for the entropy density as function of temperature for a gluon plasma from Ref. 10.

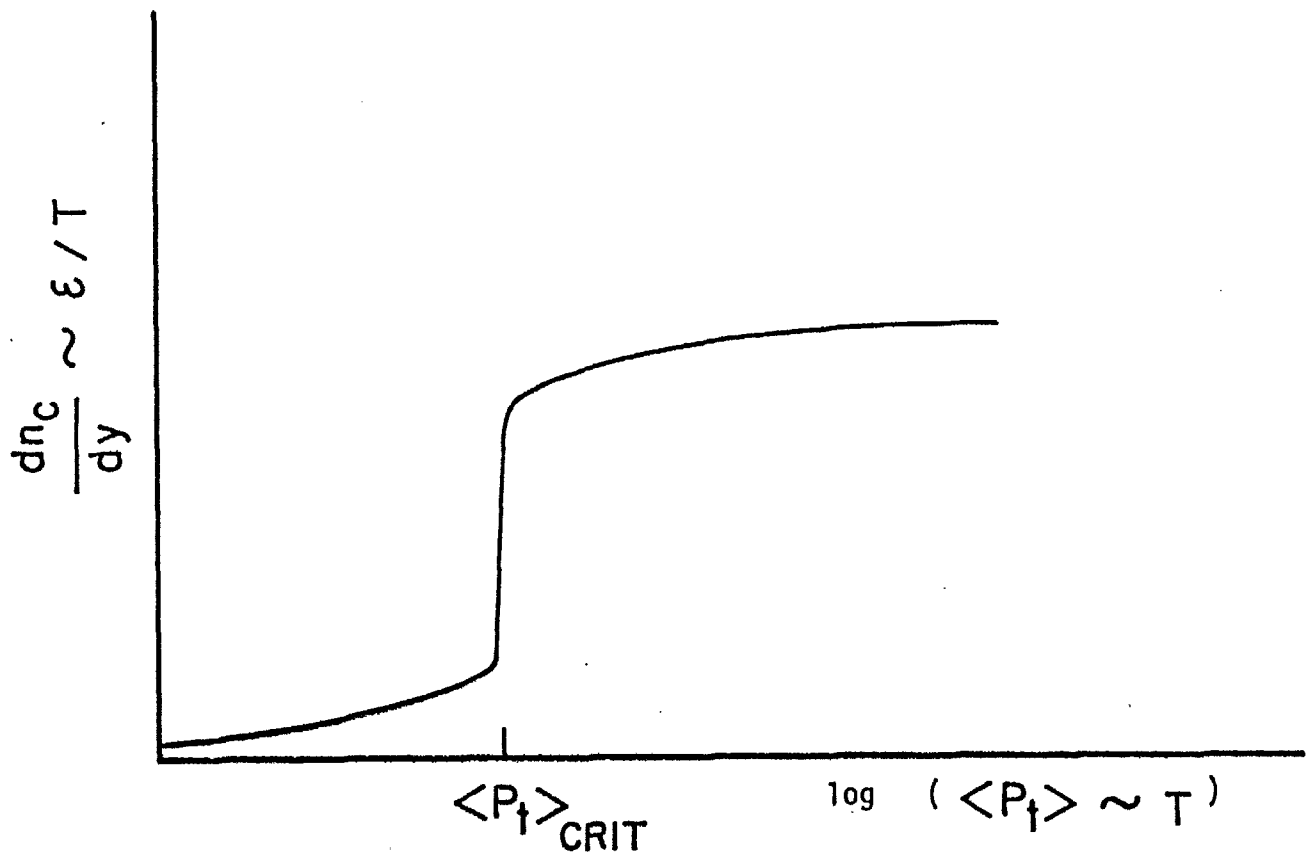

Fig. 3. Theoretical expectation of the dependence of the average transverse multiplicity on particle density in the rapidity space.

II. Motivation for the Experiment

A. Hadrons Emerging from the Quark-Gluon Plasma

To study the central region of $\bar{p}p$ collisions in the DØ area of the Fermi National Accelerator Laboratory at a center of mass energy of 2 TeV, we propose using a pair of low momentum magnetic spectrometers with particle identification. We will measure the transverse momentum (p_t) distribution of centrally produced $p^{\pm}, k^{\pm}, \pi^{\pm}, e^{\pm}$, for $p_t < 1.0$ GeV/c as a function of the charged multiplicity $n_c = \int (dn_c/dy)/dy$.

It has been observed[12] at the CERN $\bar{p}p$ collider ($\sqrt{s} = 0.54$ TeV) that the number of charged particles in the central region is larger than those observed at ISR energies, and that there exists a clear dependence of $\langle p_t \rangle$ in the central region on the central multiplicity n_c.[9]

It has been pointed out[8] that this increase in $\langle p_t \rangle$ as a function of n_c could indicate the combined effect of transverse expansion and temperature caused by the energy which has been deposited in the central region. The $\langle p_t \rangle$ versus particle multiplicity is shown in Fig. 4.

As seen in Fig. 4, the increase of $\langle p_t \rangle$ with dn/dy is the same at the CERN-collider, the ISR, and for fixed target Fermilab data for the common range of dn/dy. Figure 4 shows a cessation of the rise in $\langle p_t \rangle$ with increasing dn/dy which is compatible with a phase transition; that is, as the entropy density ($\varepsilon/T \propto dn/dy$) continues to increase the temperature ($T \propto \langle p_t \rangle$) remains constant. From data at a single $\sqrt{s}$ we cannot rule out that this is merely a kinematic effect. It is therefore important to repeat this measurement at $\sqrt{s} = 2$ TeV where the range of dn/dy is at least 1.5 times as great simply from the ln(s) effect. Since the CERN-collider experiments[22] have reported (Fig. 5) an excess of high multiplicity events as compared to a KNO scaling curve (or in comparison to ISR) the assumed $n_c \sim \ln(s)$ underestimates the available dn/dy range at Fermilab.

Our group has studied pion production in the central region[13] in pp collisions at $\sqrt{s} = 7.7$ GeV. The observed p_t distribution can be quantitatively interpreted in terms of a thermodynamic picture where the

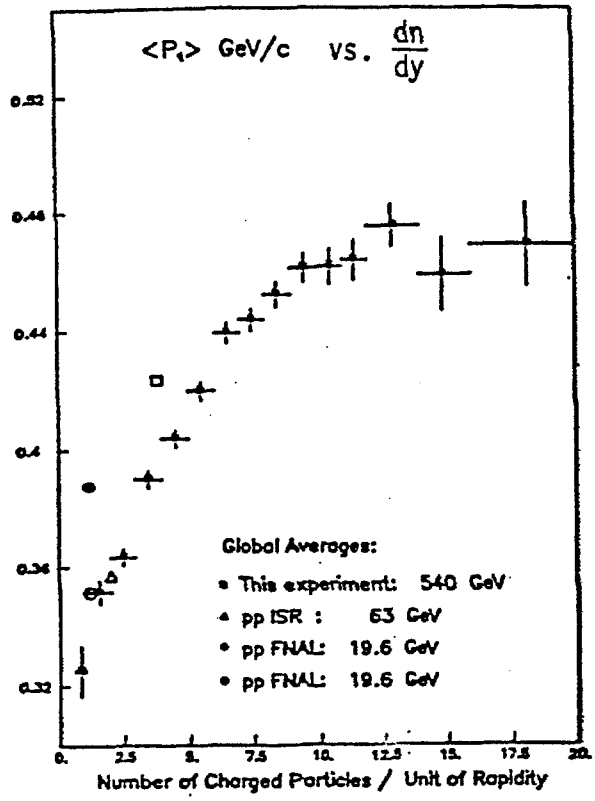

Fig. 4. The mean transverse momentum of charged hadrons ($\sqrt{s}$ = 540 GeV) as a function of charged track multiplicity in the rapidity interval $|y| < 2.5$. (Error bars are purely statistical.) From Ref. 9. To be compared with Fig. 3 (interchange x,y variables).

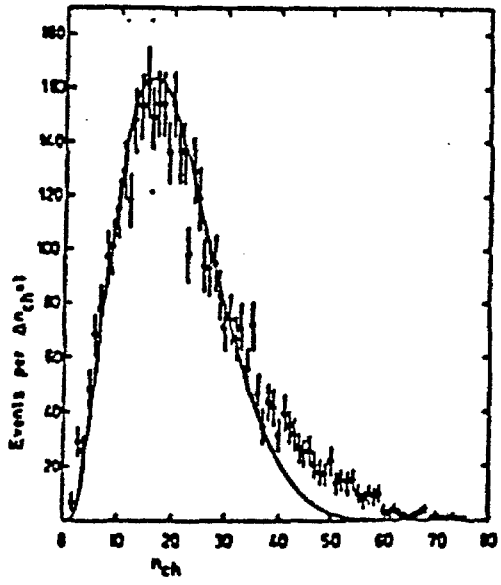

Fig. 5. The distribution of observed charged multiplicities in the UA5 experiment. Errors shown are statistical. The curve is a fit to lower energy data and scaled to $\sqrt{s}$ = 540 GeV. From Ref. 22.

distribution dn/dp_t yields a Bose-Einstein statistical distribution from which a temperature of 117 MeV can be extracted. The fit to the data is shown in Fig. 6. Other authors have found similar values for the temperature of nuclear matter at SLAC,[14] FNAL[15] and ISR[16] energies.

In our work,[13] the determination of T = 117 MeV involved 4, 6, 8 and 10 prong events. If we assume that $\bar{n}_c = 5$ for these events this corresponds to $\frac{d\bar{n}_c}{dy} \sim 1.3$. Accepting the thermodynamical relations, which hold outside the region of phase transition;

$$\frac{dn}{dy} \propto T^3$$

we can estimate the critical value of dn/dy as follows:

$$\frac{\left(\frac{dn_c}{dy}\right)_{crit}}{1.3} = \left(\frac{T_{crit}}{117}\right)^3 = \left(\frac{215}{117}\right)^3$$

From which we obtain

$$\left(\frac{dn_c}{dy}\right)_{crit} = 8$$

The subscripts "c" and "crit" denote charged and critical, respectively. We also made use of the theoretically predicted $T_{crit} = 215$ MeV.

An independent estimate of the energy density, ε, in the central region using a one dimensional model is given in Appendix I.

As shown in Fig. 4, the mean transverse momenty $\langle p_t \rangle$, at $\sqrt{s} = 0.54$ TeV has been measured as a function of dn_c/dy in the range 1 to 15 and indeed it is observed that $\langle p_t \rangle$ becomes a constant for $\frac{dnc}{dy} > 8$. This indicates that temperatures on the order of twice those attainable at $\sqrt{s} = 7.7$ GeV may just be reached at $\sqrt{s} \sim .5$ TeV. However, the experiment needs to be done at higher energies to rule out kinematic effects, i.e. lack of energy and with much higher statistics. The flattening of $\langle p_t \rangle$ has also been detected for very complex events by the Brazil-Japan cosmic ray collaboration.[17]

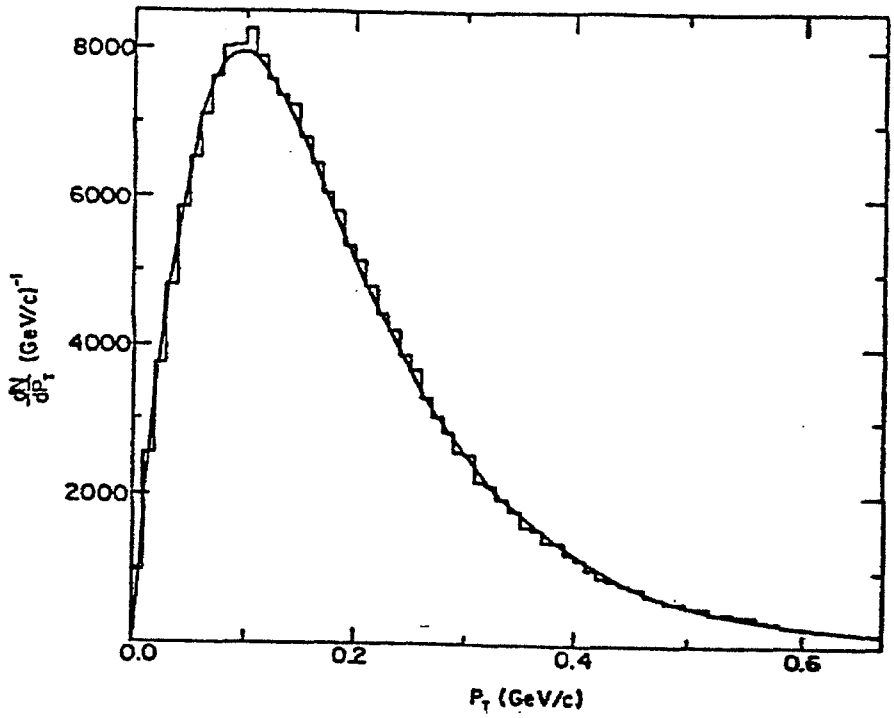

Fig. 6. The transverse-momentum distribution for central particles in the asymptotic large-multiplicity limit in the reaction $p_1 + p_2 \rightarrow p_3 + X$. The curve is a fit to the Bose-Einstein statistical distribution. From Ref. 13.

B. Dileptons Emerging from a Quark-Gluon Plasma

So far we have discussed how a quark-gluon plasma would manifest itself by emission of strongly interacting particles. An alternate signature would be the production of low mass lepton pairs. The mechanism is $\bar{q}q$ annihilation into leptons;

$$q + \bar{q} \rightarrow e^+ + e^- \quad .$$

The importance of this reaction for quark matter diagnostics has been discussed by Domokos.[18] The cross sections for dilepton pairs will be suppressed by α^2 compared to the strong interaction rates. A rough estimate that takes into account the thermal motion of quarks in the plasma by Domokos derives the temperature and invariant mass dependence of the dilepton production.[18] Using his formulae we estimate that the dilepton rate in 200 MeV < $m_{e^+e^-}$ < 600 MeV mass range is about 0.5 percent of the event rate for the dn_c/dy = 25 events with $T \sim 200$ MeV. They are expected to be isotropic in the rest frame of the plasma and have a low ($m_{e^+e^-}$ < 600 MeV) effective mass.

A competing process to $\bar{q}q < e^+e^-$ is the

$$\pi^+ + \pi^- \rightarrow e^+ + e^- \quad .$$

The relative rates are shown in Figs. 7a and 7b from Ref. 18.

Our double arm spectrometer is well suited for detecting e^+e^- pairs when they are produced with the thermal energy of $2T \approx 400$ MeV back to back. According to Ref. 18 the low mass (200 MeV < $m_{e^+e^-}$ < 600 MeV) is dominated by the $\bar{q}q \rightarrow e^+e^-$ process and the corresponding lepton momenta are such that both our hadron data can be collected concurrently with the dilepton events. The advantage of the dilepton channel is that they can be emitted by the plasma any time during its lifetime.

C. Centauro Events

The number of "unusual" events which may be observed at $\sqrt{s}$ = 2 TeV can be estimated from cosmic ray data if it is assumed they are initiated by a $\bar{p}$-p collision.[17] A translation in terms of center of mass energies is shown in Fig. 8.

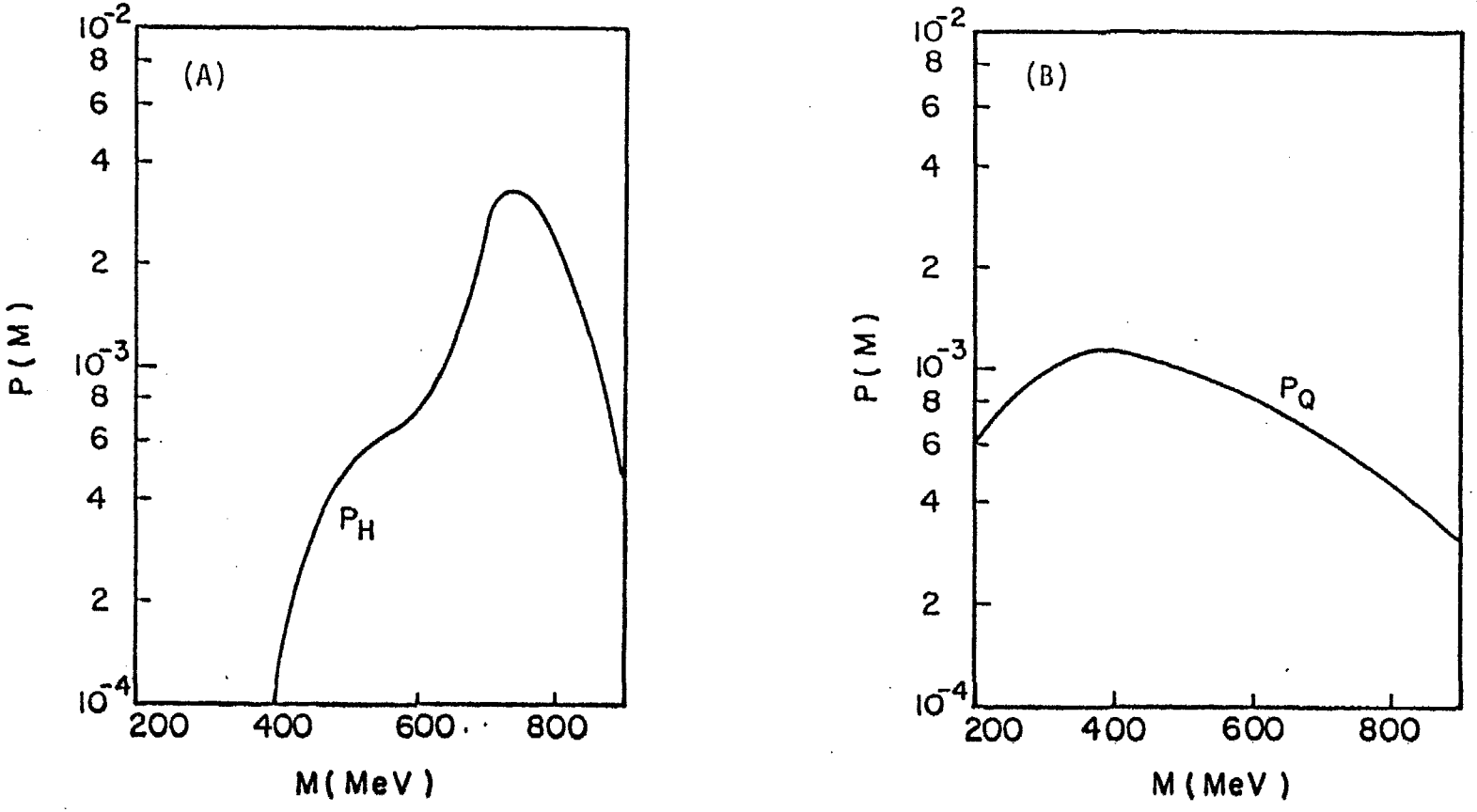

Fig. 7. Normalized dilepton roles for (A) $\pi^+ + \pi^- \to e^+ + e^-$ and (B) $\bar{q} + q \to e^+e^-$. Ref. 18.

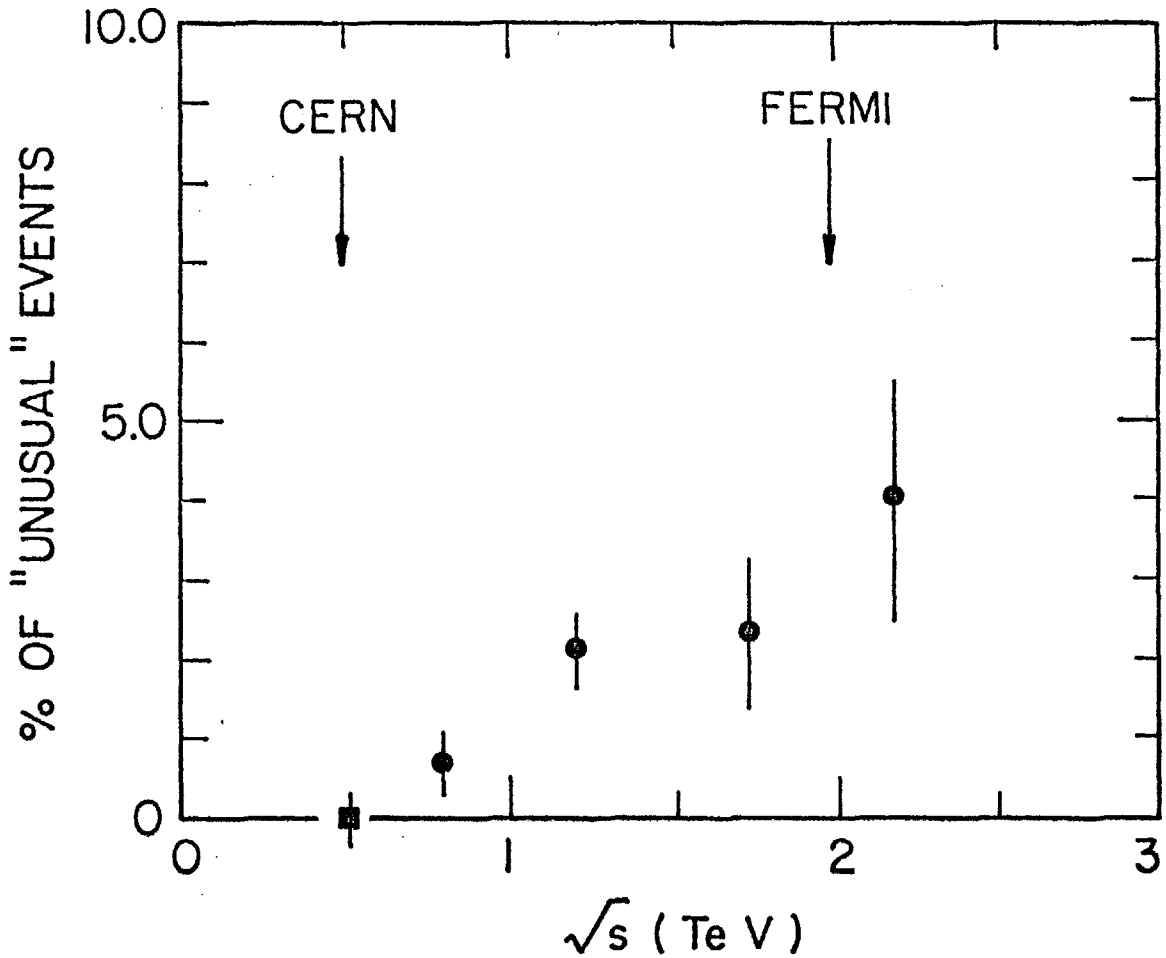

Fig. 8. The number of unusual events as function of the center of mass energy from Ref. 17.

These $\sqrt{s}$ values are somewhat uncertain because they depend on the estimates of the energy of the primary p-p collision. The signature of these Centauro events is characterized by a large number of hadrons $n_c \sim 75$ and a number of gamma rays n_γ consistent with zero. Thus it is possible to search for this type of event if we are also sensitive to the number n_γ, provided that the particles emerge in the central region. Since Centauro events have only been observed in cosmic ray experiments, both the interaction point and the dn/dy for these events are unknown as discussed in Ref. 19. If the decay product emerge dominantly in the central region we would measure about 30 charged hadrons with a number of n_γ consistent with zero. Any associated particles $|y| \leq 1$ would be observed in our charged particle spectrometer. We would expect that such a spectacular signature which could be due to dominant baryon-antibaryon production could be seen if these events were more numerous than the fluctuations of n_γ expected for the normal events which are dominated by pion production.

III. Experimental Layout

A. Central Region

The top view of the experimental apparatus is shown in Fig. 9a. In the central region $|y| \leq 3$ the n_c and n_γ multiplicities are determined by a five layer cylindrical proportional wire chamber CWPC, a cross section of which is shown in Fig. 10, and the end cap arrays. The details of the CWPC are presented in Appendix II. In the first level of reconstruction only the inner three layers of the wire chambers are used. The individual particles which have been observed in the magnetic spectrometers must arise from this vertex.

Since we are interested in events whose charged multiplicities are up to five times the average n_c, we must distinguish between a single high multiplicity interaction and the occurrence of two independent lower multiplicity events in the same collision pulse. Reconstruction of the vertex or vertices will allow us to resolve two different vertices which are more than one cm apart along the beam direction. For a collision pulse width FWHM of 50 cm this means we can reduce this accidental background by a factor of 50. At low ($10^{27}cm^{-2}sec^{-1}$) luminosities accidentals are not a problem. At high luminosities ($10^{29}cm^{-2}sec^{-1}$) reconstruction of the event is an essential feature.

The fourth and fifth outer layers of the CWPC are used to detect the gammas (n_γ) converted in the lead and to give a crude photon direction. Since $n_\gamma \sim n_c$ we should get an excellent indication that for these events $\langle n_\gamma \rangle \sim \langle n_c \rangle$. Apertures in the converter are provided so that low momentum particles can be seen by the magnetic spectrometers. Of course only for non-Centauro events is it expected that $n_\gamma \sim n_c$.

The dimensions of the low momentum spectrometers are shown in Fig. 9b. The traditional design has a pseudorapidity acceptance of $|y| \leq 1$ and an azimuthal range $\Delta\phi$ which assures that about one particle is detected when the multiplicity is $n_c = 35$. The magnetic gaps are 75 inches long, 10 inches and 5 inches deep as seen from the interaction region. The double gap magnet, which is detailed in Appendix III has copper coils and an iron return path. The five cylindrical chambers determine the incident particle direction θ_1, three drift chambers behind the magnet the final

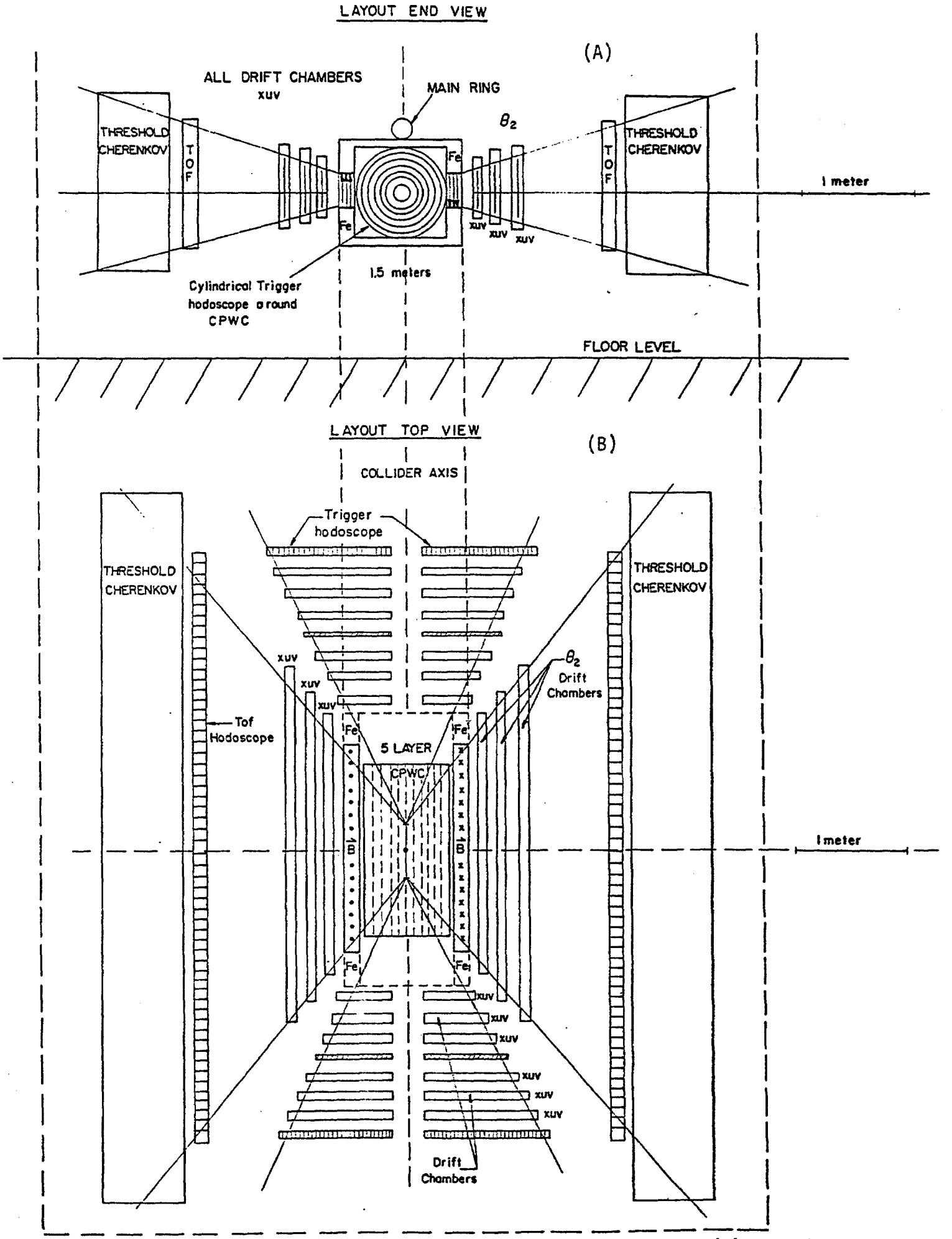

Fig. 9. Layout of the experimental apparatus; (A) end view and (b) top view.

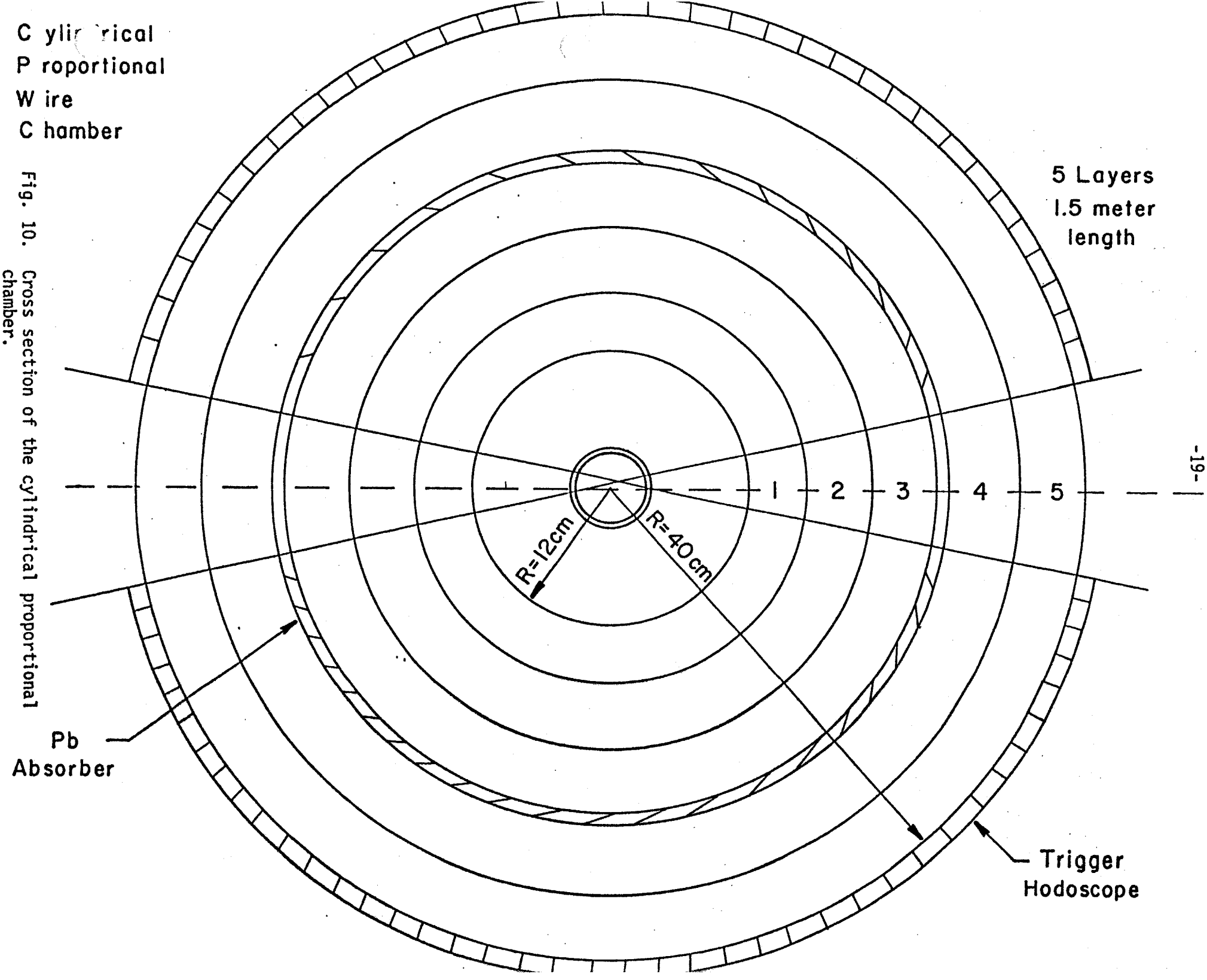

Fig. 10. Cross section of the cylindrical proportional chamber.

particle direction θ_2. Time of flight of the particle is measured by the large 1.0 meter × 6 meter hodoscope located about 2 meters from the intersecting region. For a 2 meter flight path it will be possible to identify charged electrons, pions, kaons, and protons over a momentum range of $0.1 \leq p_t \leq 1.0$ GeV/c. We have designed a threshold Cerenkov counter that can separate the electrons from muons and hadrons. The threshold Cerenkov counter (see Appendix IV) is segmented so that ambiguities due to several particles traveling through the spectrometer are eliminated.

Table I

Specifications of the magnetic spectrometer.

Quantity	Symbol	resolution (nominal)
momentum resolution at 1 $\frac{\text{GeV}}{c}$	$\frac{\Delta p}{p}$	3%
time resolution	Δt	$\sim$ 400 ps
flight path	ℓ	2 meters
probability of observing one particle of $\langle n_c \rangle$ for $\lvert y \rvert \leq 1.3$	$\frac{\Delta\phi}{2\pi}\frac{dn}{dy} \cdot y$	$\frac{1}{4}\frac{dn}{dy}$
pion proton time difference at $P_t = 1.0$ GeV/c	Δt	2.1 ns

The expected performance of this spectrometer is in line with the published results of the Argo low momentum spectrometer[20] and the CERN UA2 particle spectrometers.[21] The magnet has been designed so that adequate homogeneity of the $\vec{B}$ field is obtained and that uncertainties in the fringe field does not interfere with the event reconstruction and the operation of the accelerator. The detailed structure of the drift chambers and hodoscopes of this low momentum spectrometer are presented in Appendix IV.

B. "End Caps"

The "end cap" multiplicity counters are 6 layers of drift chambers. The inner three chambers count the charged particle multiplicity n_c. We can translate the pseudorapidity range $|y| \geq 9.2$ for Centauro events to the center of mass at $\sqrt{s} = 2$ TeV and find the kinematical range is about $|y| \geq 2$. The pseudorapidity range $2 < |y| < 3.5$ is covered by a rectangular array whose area is about one square meter. Using the observed rapidity distribution at the CERN collider at $\sqrt{s} = 0.54$ TeV,[21,22] we estimate that of the $n_c = 75$ expected for $|y| \geq 2$ we would observe 25 charged particles in both end caps. The neutrals are converted by an absorber after the third layer and counted by the outer three layers. Since for a multipion event $n_\gamma \sim n_c$ a clear signature would result for $n_\gamma \sim 0$. The details of these chambers are in Appendix V.

C. Trigger Hodoscope

A single layer scintillation hodoscope surrounds the CPWC and the outer layer of the end caps. A fast nanosecond trigger for a multiparticle event $n_c \geq n_{max}$ selects out events whose transverse momentum is $\sim 0.6\ n_c$ Gev/c.where n_{max} denotes the value at which the multiplicity distribution peaks in Fig. 5. For $n_c = 35$ this would correspond to a transverse momentum of ~ 20 GeV/c or about 20% of the highest transverse momentum event of 100 Gev/c which we could study.

A second function of the end cap trigger hodoscope is to select out those charged and neutral particle tracks in the drift chamber which are in fast coincidence with the trigger hodoscope around the CPWC. This will serve to reduce background tracks by a factor

$$\frac{t_{drift}}{t_{coincidence}} = \frac{300}{15} = 20 \quad .$$

IV. Counting Rates

The charged particle multiplicity distribution observed at the CERN collider ($\sqrt{s}$ = 0.54 TeV) by the UA5 apparatus[22] is shown in Fig. 5. At $\sqrt{s}$ = 2 TeV we expect a total cross section of above 65 mb. The inelastic cross section is expected to be 50 mb. If we assume that the distribution of charged particles does not change radically for $\sqrt{s}$ = 2 TeV then the number of events that are five times the most probable multiplicity is about 10^{-4} n_{max}. Since n_{max} should scale according to $a_0 + a_1 \ln s + a_2(\ln s)^2$, at $\sqrt{s}$ = 2 TeV we expect n_{max} = 35; about 67% of these will be within the coverage of our detector. To obtain a good value for $\langle P_t \rangle$ for a given bin of n_c, we want $\sim$2000 events in the dN/dP_t distribution; hence for 2000 events at $n_c = 5n_{max}$, we would have 3×10^8 total events for a minimum bias trigger. If we assume that we are exposed to a luminosity of $L = 10^{27}cm^{-2}sec^{-1}$ at DO for 10^7 secs, the total number of events N is; $N = 10^{27}cm^{-2}sec^{-1} \times 50$ $10^{-27}cm^{-2}sec^{-1} \times 10^7 sec = 5 \times 10^8$ events. Hence a run of 10^7 sec is quite adequate; clearly we must heavily scale down the number of events accepted at low multiplicity in order to limit the total data sample to a manageable number, e.g. 2×10^6 events.

We can simply estimate the double interaction problem. The probability of a single interaction is a collision pulse for $L = 10^{27}cm^{-2}sec^{-1}$ is

$$\frac{50/sec}{140{,}000/sec} = 3.6 \times 10^{-4} .$$

The probability of a real event with multiplicity 2 n_{max} is 3.6×10^{-5}. We would expect an accidental double vertex background rate of $(3.6 \times 10^{-4})^2$ or 3% of the real rate. For $L = 10^{28}cm^{-2}sec^{-1}$, this would rise to 30%. However tracking through the cylindrical chambers would further reduce this by a factor of 50, i.e., 0.6% of the real rate.

V. Cost Estimate

An itemized cost estimate is given in Appendix VII; it sums up to 1.5 M$.

References

1. E. Fermi, Prog. Theor. Phys. 5, 570 (1950).

2. L. D. Landau, Izv. Akad. Nouk. S.S.S.R. 17, 51 (1953).

3. M. Gell-Mann, Synchrotron Laboratory Report CTSL-20 (1961); M. Gell-Mann, Phys. Lett. 8, 214 (1964); C. Zweig, CERN Report Nos. TH 401, 402 (1964).

4. J. D. Bjorken, Phys. Rev. 179, 1547 (1969); J. D. Bjorken and E. A. Paschos, Phys. Rev. 185, 1975 (1969); S. J. Drell, D. J. Levy and T. M. Yan, Phys. Rev. Lett. 22, 744 (1969).

5. D. Gross and F. Wilczek, Phys. Rev. Lett. 30, 1343 (1973); H. D. Politzer, Phys. Rev. Lett. 30, 1346 (1973).

6. H. Georgi and H. Politzer, Phys. Rev. D 14, 1829 (1976).

7. L. D. McLerran and B. Svetitsky, Phys. Lett. 98B, 199 (1981); J. Kuti, J. Polonyi and K. Szlachanyi, Phys. Lett. 98B, 199 (1981).

8. L. Van Hove, Phys. Lett. 118B, 138 (1982); J. D. Bjorken, Fermilab Pub. 82/44-THY.

9. UA1 Collaboration, Phys. Lett. 118B, 167 (1982).

10. J. Engels et al., Nucl. Phys. B205, 545 (1982).

11. J. Kogut et al., University of Illinois (Urbana) preprint ILL-(TH)-82-39, November (1982).

12. J. G. Rushbrook, Proc. of the 21st Int. Conf. on High Energy Physics CS-111.

13. A. T. Laasanen et al., Phys. Rev. Lett. 38, 1 (1977).

14. J. Erwin et al., Phys. Rev. Lett. 1534, 27 (1971).

15. D. Brick et al., Nucl. Phys. B152, 45 (1979).

16. T. F. Hoang, Phys. Rev. D 8, 2315 (1973).

17. C. M. G. Lattes, Y. Fujimoko and S. Hasegawa, Phys. Rep. 65, 152 (1980).

18. G. Domokos and J. L. Goldman, Phys. Rev. D 23, 203 (1981); G. Domokos, JHU-HET 8212 (1982); G. Domokos, JHU-HET 8301 (1983).

19. UA1 Collaboration, Phys. Lett. 122B, 189 (1983).

20. E. W. Anderson et al., Nucl. Inst. and Meth. 122, 587 (1974).

21. J. P. Rapellin, CERN UA2 Collaboration, Proc. of the 21st Int. Conf. on High Energy Physics C3-571; M. Banner et al., Phys. Lett. 122B, 322 (1983).

22. P. Carlson, CERN UA5 Collaboration, Proc. of the 21st Int. Conf. on High Energy Physics C3-593.

Appendix I
Estimates of the Energy Density

We can estimate the energy density in the central region using a one dimensional model.[1] Consider a section of outgoing matter

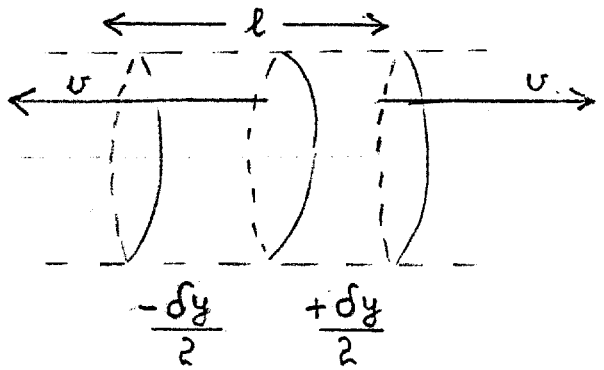

The volume of the cylinder $A \times \ell$ where

$$\ell \simeq 2vt \simeq t\delta y$$

where in the non-relativistic approximation

$$2v = \delta y$$

Let be the energy density and $A = \pi r^2$

$$\varepsilon = \frac{1}{A \times \ell} \frac{dE_A}{dy} \delta y \qquad \varepsilon = \frac{1}{t\pi r^2} \frac{dE_A}{dy}$$

t may be thought of as the lifetime of the thermalized blob. We can use experimentally determined values for pp collisions at $\sqrt{s}$ = 7.7 GeV.[2] Here t = 2fm and r_{11} = 0.7 fm. We assume $r_{11} \geq r_{\perp}$

$$t = 2 \text{ fm} \qquad r_{11} = 0.7 \text{ fm}$$

For pions

$$\frac{dE_A}{dy} \sim (0.4 \times \frac{3}{2}) \frac{dn_c}{dn}$$

where the 3/2 factor includes the contributions from π^0 mesons. Finally for

$$\frac{dn_c}{dy} = 8$$

$$\varepsilon = \frac{0.6}{2 \times \pi\ (0.7)^2} \qquad 8 \sim \frac{1.6\ \text{GeV}}{\text{fm}^3}$$

Studying high transverse energy events Bjorken argues[3] that energy densities substantially greater than our estimates may have been already observed at the CERN $\bar{p}p$ collider.

References to Appendix I

1. J. D. Bjorken, Fermilab Pub.-82/44 THY.
2. C. Ezell et al., Phys. Rev. Letters 38, 873 (1977).
3. J. D. Bjorken, Fermilab Pub.-82/59 THY.

Appendix II

The Sizes, Wire Spacings and Wire Counts of Wire Chambers

1. The end cap drift chambers (xuv)*

Width (cm)	Wire spacing (cm)	Number of wires	Double hit capability
50	1	50	yes
55	1	55	yes
60	1	60	yes
80	2	40	yes
90	2	45	yes
95	2	47	yes

Total number of wires = 3 × 4 × 300 = 3600

N^E_{total} = 3600 wires length = 2 meters

2. The transverse drift chambers (xuv)*

Width (cm)	Wire spacing (cm)	Number of wires	Double hit capability
230	2	115	no
275	2	137	no
320	2	160	no

Total number of wires = 3 2 412 = 2472

N^T_{total} = 2472 wires length = 1 meter

3. The central cylindrical proportional chambers

Circumference (cm)	Wire spacing (cm)	Number of wires	Charge division
70	0.15	466	yes
105	0.20	525	yes
140	0.20	700	yes
175	0.20	870	yes
250	0.10	1250	yes

N^C_{total} = 3811 wires length = 1.5 meters

*u,v are rotated by ±16° with respect to x.

To determine the location of the hit along the wire of CPWC we will use charge division. To improve the conventional resolution we will investigate the possibility of operating our chambers in a self-quenching streamer mode.[1] This may improve the resolution by a factor of 10.

References to Appendix II

1. M. Atac, A. V. Tollestrup and D. Potter, Nucl. Inst. and Meth. 200, 345 (1982).

Appendix III

The Dimensions and Counts of Trigger Hodoscopes

1. The end cap trigger hodoscopes vertical

	Hodoscope width (cm)	Cross section (cm^2)	Number of segments	Light division
Vertical	100	2 × 1	50	yes
Horizontal	200	4 × 1	50	no

Total number hodoscope elements = 4 × 100 = 400

Vertical element length = 2 meters

Horizontal element length = 1 meter

2. The time of flight hodoscope

	Hodoscope width (cm)	Cross section (cm^2)	Number of segments	Light division
Vertical	530	5 × 2	106	yes

Total number of hodoscope elements = 2 × 106 = 212

Vertical element length = 1 meter

3. The trigger hodoscope on the cylindrical chamber

	Hodoscope radius (cm)	Cross section (cm^2)	Number of segments	Light division
Horizontal barrel	43	4 × 1	68	no

Total number of hodoscope elements = 68 × 2 = 136

Horizontal element length = 1.6 meters

Appendix IV
Parameters of the Spectrometer Magnet

The spectrometer magnet, whose vertical cross section (perpendicular to the beam) is shown in Fig. 11, consists of a pair of dipoles centered at 20" on either side of the beam. The four coils are connected in series such that the fields in the two 10" gaps are anti-parallel; this configuration allows the two magnets to share a common flux return path. The symmetry around the Tevatron beam ensures zero magnetic field there; field gradients, such as quadrupole and octopole, will exist but are expected to be manageable. The Main Ring beam is 3" above the top of the magnet yoke, allowing adequate space for magnetic shielding of the small fields that will exist there.

The mechanical parameters of the magnet are:

Yoke outer dimension, x:y:z = 45" × 45" × 76"
Gap height = 10", pole width = 5"
Coil cross section, x:y = 2 1/4" × 6 1/2"
Weight of iron = 5.6 t
Weight of 4 coils = 1.4 t
Angular acceptance: $\Delta\phi$ = 25°
$\Delta\theta$ = ±59° (n = ±1.3)

The magnet is designed to give a transverse deflection of 40 MeV/c to a particle traveling at 0 = 90°. The magnetic and electrical parameters corresponding to this are:

Field at gap center = 3.5 kG
Coil current density = 3 ka/in
Power dissipation = 50 kw
Magnetic field in yoke = 7 kG

If the coils were wound with water cooled copper bus similar to that used in Main Ring dipoles (0.9 in^2 of copper), each coil would have 12 turns, yielding a magnet voltage of 17V. We estimate the total cost of the magnet to be 45K$.

MAGNET VERTICAL SECTION

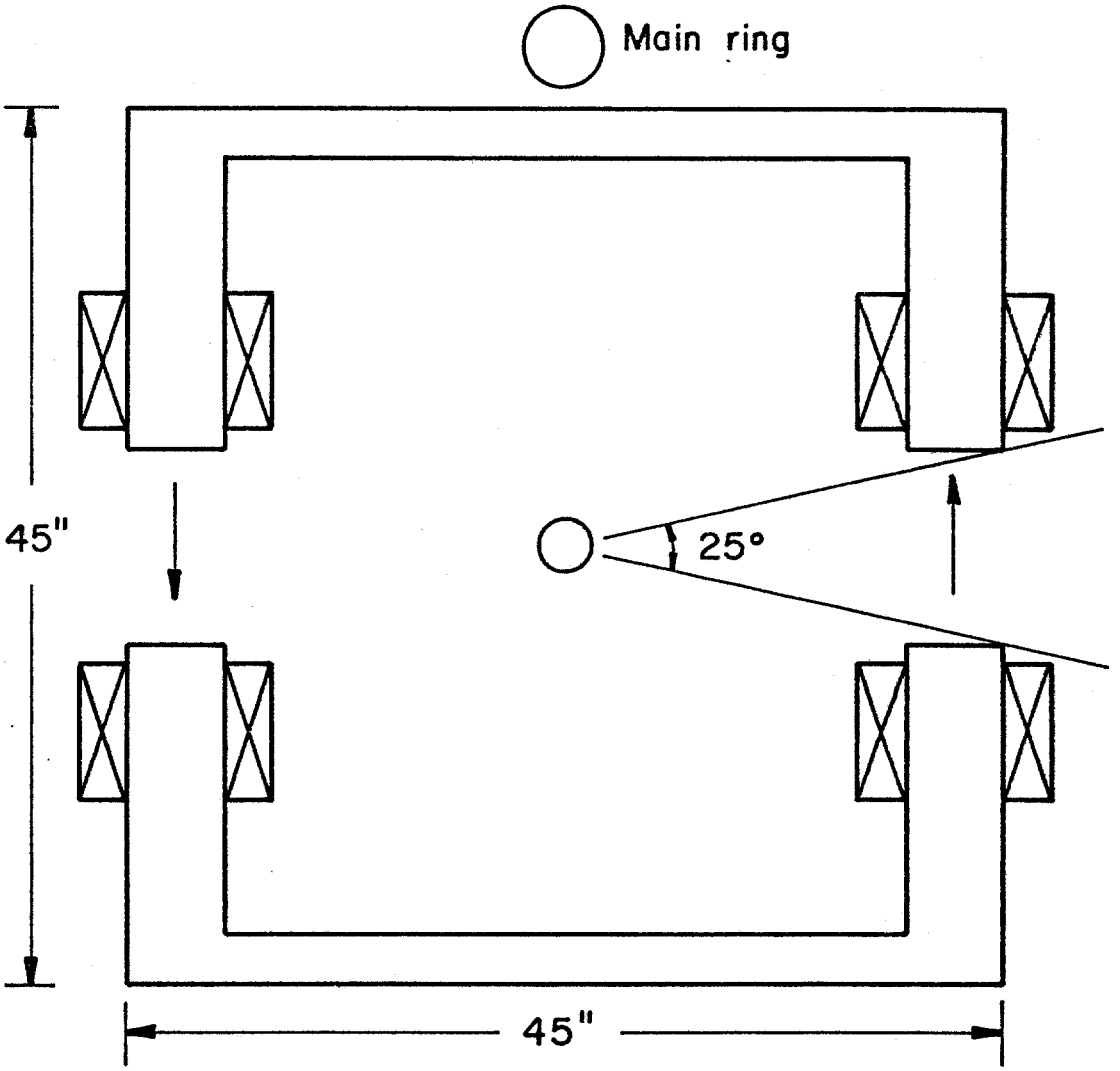

MAGNET TOP VIEW

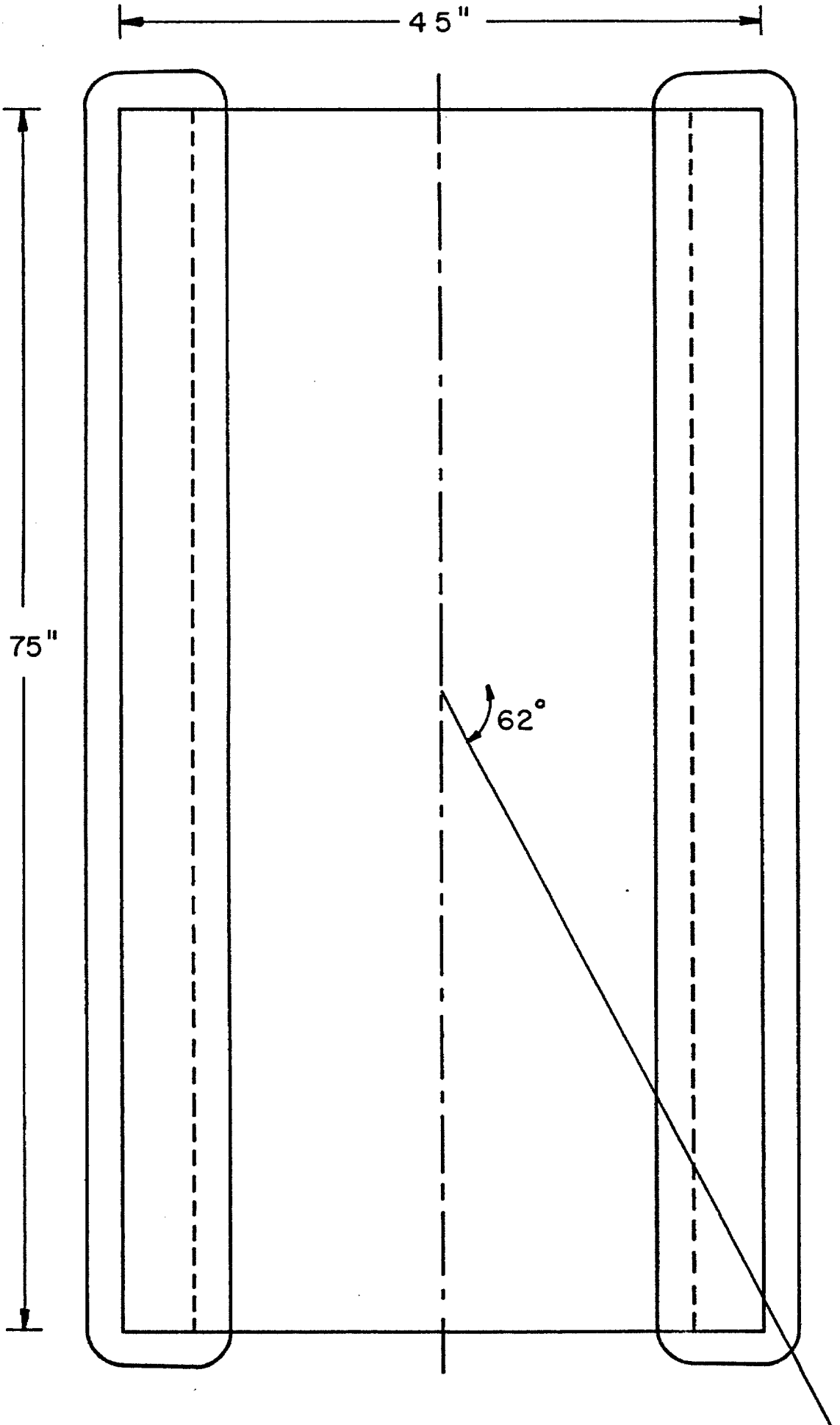

Appendix V
Description of the Cherenkov Counter

The threshold Cerenkov counters are atmospheric pressure room-temperature Freon-12 filled vessels. As the index of refraction is of Freon is 1.0011, only electrons are above threshold in the momentum range 10 MeV/c to 3 GeV/c. The Cerenkov counters are 1.5 meters deep, so that the expected number of usable photons is 130. These photons are highly collimated. The back dimensions of the counter are 2m by 9m and can be covered by 18 spherical mirrors (with clipped edges). These mirrors will be arranged so as to throw the light back to 18 phototubes (5 inch) arranged along the top and bottom of the front Cerenkov wall. We will use 5" RCA quantacon low noise phototubes (PT) or their equivalents. An example of mirror arrangement is shown below.

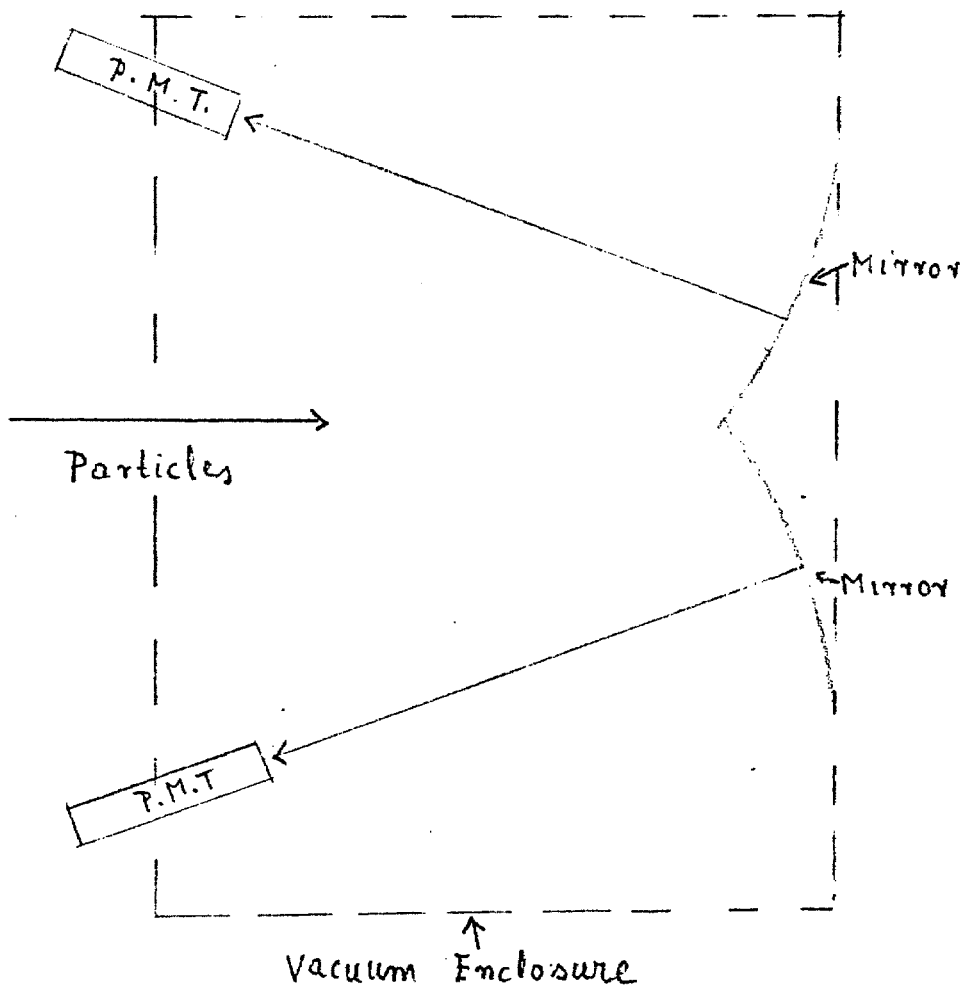

Appendix VI
Background Considerations

A. CPWC and End Cap Wire Chambers

Our experience in E591 with semiconductor detectors operating $\sim$ 30 cm from the main ring beam pipe indicates a flux of $\sim 10^4/cm^2 sec$ minimum ionizing particles during the acceleration cycle of 10^{13} protons when the gas jet was not in operation. This means that a single drift chamber cell of area 200 cm^2 would sustain about one hit during the $\sim$ 0.5 μs drift time. Consequently, double hit capability is required on the end cap drift chambers. In addition the following precautions were taken: (a) One vertical scintillator rod backs up each cell of the last drift chamber. (b) Each vertical rod is equiped with photomultiplier tubes on each end to ensure light division capability. The above features make it possible to recognize the time correlated hit in the drift chamber cell, as by the time zero pulse from the central hodoscope. Thus background hits can be reduced by a factor of 500 n·s/10 n·s = 50.

We expect that this is a worse case argument, namely only 5 · 10" particles are circulating in the collider ring, the vacuum is much better and the beam is coasting. It is our understanding that the CERN SPS experience indicates that the background is indeed less than the estimates we have made based on the C_0 experience.

B. Lepton Pair Background

To reduce the lepton background we have to minimize the mass of the beam pipe and the walls of the CPWC so that only a minimum number of gamma rays are converted. If the beam pipe is constructed of 25 mil Be and the walls of the CPWC are aluminized mylar then it is reasonable to say that gamma rays see less than 10^{-2} of a radiation length. Further rejection of these events is provided by reconstruction of the pair events in the CPWC. An additional drift chamber in the magnetic field can be used to observe low $\leq$ 40 Mev/c momentum leptons. A background event would occur. When only one lepton from a pair is seen in each spectrometer, they are of opposite sign and have a low 200 - 600 Mev/c invariant mass. Thus it is

essential to be able to observe both leptons of pair in a high percentage of the events.

An additional source of background events are produced by energetic particles which strike the magnet yoke etc. We would use event reconstruction to eliminate these events the more accurately we are able to determine the interaction vertex the better the rejection factor. The use of the self-quenching streamer mode of operating the CPWC charge division would improve vertex resolution by a substantial factor.

C. Jet Events

Order of magnitude estimates[1] of the cross section for the production of a particle jet are $\sigma \sim 10^{-30}$cm when the transverse momentum P_t of the jet is 10 Gev/c. Since we are interested in events where $\sigma \sim 5 \cdot 10^{-26}$ for $n_c \sim 35$ to $\sim 5 \cdot 10^{-30}$ for $n_c = 175$. We must depend on event reconstruction to reject jet events. Such a jet would have several particles with a small $\leq 20°$ opening angle. We should be able to distinguish this type of event from a high multiplicity central event. Higher P_t jets have much lower cross sections.

Reference for Appendix VI

1. Design report for the Fermilab collider CDF, August 1981, page 40.

Appendix VII
Cost Estimates

		In Thousands
1.	End cap drift chamber electronics, LeCroy T.D.C. 3600 wires with double hit capability	324.0
2.	Transverse drift chamber electronics, LeCroy T.D.C. 2472 wires	123.6
3.	Central cylindrical proportional chamber electronics with charge division, LeCroy 0.1 pico coulomb / channel A.D.C. 3811 wires, 2 channels ea required	404.0
4.	Trigger hodoscope for end cap 400 element, 200 required with light division	60.0
5.	Trigger hodoscope for central chamber 126 elements	12.6
6.	Time of flight hodoscope, 212 elements with light division	424.0
7.	Cherenkov Counter, 36 light collection segments, R.C.A. 8854 quanticon	72.0
8.	Magnet iron and coils	45.0
	Total	1465.2 K